

Research Article

Vol No: 05, Issue: 01

Received Date: Mar 09, 2020

Published Date: May 14, 2020

Quanshi Zhang¹

Guiping Xiao¹

Qiyin Sun¹

Jun Zeng¹

Liang Wang¹

Lili Chen²

Chang-Ming Charlie Ma^{2*}

¹Radiotherapy Centre, Wuxi Yiren Tumor Hospital, Beijing, 100176, China

²Department of Radiation Oncology, Fox Chase Cancer Center, Philadelphia, PA 19111, USA

Corresponding Author:

Chang-Ming Charlie Ma*

Department of Radiation Oncology, Fox Chase Cancer Center, Philadelphia, PA 19111, USA.

E-mail: Charlie.Ma@fccc.edu

Investigation of the Mechanisms of Radio-Dynamic Therapy

ABSTRACT

Purpose: Photodynamic therapy (PDT) uses light-activated drugs to treat diseases ranging from cancer to age-related macular degeneration and antibiotic-resistant infections. The finite penetration depth of light has limited the clinical application of PDT. This work investigates the substitution of light in PDT using Cerenkov light induced by 45MV photon beams from the LA45 therapy accelerator. This new treatment technique has been named radio-dynamic therapy (RDT) and this paper investigates the dosimetric requirement of RDT.

Method: Cerenkov light and its spectrum induced by 45MV x-ray beams from a LA45 therapy accelerator, was simulated with the Monte Carlo method. The excitation efficiency of Cerenkov light in RDT was theoretically studied and compared with the excitation efficiency of external laser light in PDT. Experiments were carried out to enhance the excitation efficiency for singlet oxygen production with specific coenzymes as substrates. These results were compared with previous experimental work reported in the literature.

Results: Our Monte Carlo results showed that the intensity of Cerenkov light induced by 45MV photons from a LA45 accelerator was 5-8 times of that induced by 6MV photons from conventional radiotherapy accelerators. The excitation effect for the homogeneous internal Cerenkov light distribution induced by 3DCRT was over 10 times of that by external laser light that is nearly exponentially attenuated in conventional PDT. According to the Soret-Band resonance absorption theory, Cerenkov light induced by 45MV X-rays, which is peaked at 370 - 430nm, can be 10-20 times more effective in activating PpIX to produce singlet oxygen than the 630nm laser light used in conventional PDT. Finally, the specific coenzyme enhanced excitation efficiency by 3 times. Furthermore, RDT is delivered with 3DCRT using 45MV photons from LA45 accelerators (3- 6Gy/fraction, 1fraction/week, 4~6weeks). This fractionated radiotherapy had a synergetic effect on the outcome of Cerenkov-induced PDT.

Conclusion: Our results indicated that the light dose and fluence rate of RDT using Cerenkov light from 45MV x-rays was comparable to that in conventional PDT using the 630nm laser light. Combining the therapeutic effect of Cerenkov-induced PDT and the deep penetration and conformity of high-energy x-ray RT, RDT may be developed into a potential treatment modality for a wide range of cancers at various stages as well as for other diseases.

INTRODUCTION

Photodynamic therapy (PDT) uses light-activated drugs to treat diseases ranging from cancer to age-related macular degeneration and antibiotic-resistant infections. Over the years, PDT has developed into an important treatment modality for superficial and shallow cancers [1]. PDT involves the administration of a tumor-targeting photosensitizer or photosensitizer prodrug (e.g. 5-aminolevulinic acid [5-ALA], a precursor in the heme biosynthetic pathway) and the subsequent activation of the photosensitizer by light. The photosensitizer can accumulate selectively within tumor tissues and absorb visible light and subsequently transfer most of the absorbed energy to oxygen molecules. This process converts the oxygen into some relatively strong active oxidizing agents; such as singlet oxygen. Singlet oxygen can destroy cell structure and block the delivery of nutrition to the cell. However, due to limited visible light depth penetration (usually, the efficient treatment depth is less than 7mm), PDT has not been extensively utilized clinically.

Various methodologies and technologies have been developed to expand the clinical application of PDT [1-4]. Traditional improvements include delivery of light directly into targets via an applicator; invasive procedures, such as fiber-optic delivery in interventional therapy or endoscope-accessible light source; and intra-cavitary irradiation [5,6]. Such methods are time-consuming, invasive, and inconvenient. An additional disadvantage is the difficulty to maintain sterile conditions over a prolonged period of time. There are also novel emerging techniques that deliver light via other agents. Kotagiri N, et al. [3] used the light emitted from the ^{18}F -FDG PET tracer and Hartl BA, et al. [7] used the light emitted from the radionuclide, Yttrium-90, to activate photosensitizers and create singlet oxygen for deep tumor treatment. Although the light emitted from the ^{18}F -FDG substituted external light in PDT to kill cancer cells effectively in mice [3], the work by Glaser AK, et al. [8] indicated that the intensity of light created from the ^{18}F -FDG is very weak and currently insufficient to apply clinically. For phototherapy applications, MC simulation outcomes [8] showed that the total light dose was found to be on the order of nJ cm^{-2} for radionuclides and mJ cm^{-2} from radiotherapy beams on conventional Linacs. In a recent study by Justus A, et al. [4], psoralen was activated by UV light emitted from novel non-tethered phosphors under kV x-ray irradiation. Copper cysteamine (Cu-Cy) nanoparticle is a new type of photosensitizer that can be efficiently activated by kV x-ray or microwave to produce the singlet oxygen for cancer

treatment [9,10]. Scintillation or persistent luminescence nanoparticles with attached photosensitizers such as porphyrins are used as an in vivo agent for photodynamic therapy [11]. Upon exposure to ionizing radiation such as kV X-rays, the nanoparticles emit scintillation or persistent luminescence, which, in turn, activates the photosensitizers as porphyrins. Upconverting nanoparticles (UCNP) use similar principles but instead the near-infrared light is employed as the activation source instead of X-rays [12,13]. Although these methods have shown some positive results in vivo, the penetration depth for kV X-rays or microwaves is still limited.

Both the traditional improvements and emerging techniques have disadvantages and limitations. Therefore, research efforts have increased to develop an alternative to laser light in conventional PDT to overcome its limited penetration depth. Light emission occurs when a charged particle moves faster than the speed of light in a given dielectric medium. This phenomenon was experimentally discovered by Cerenkov PA, et al. in 1934 [14] and subsequently named Cerenkov light. At present, Cerenkov light has mainly been used in two fields of medicine: 1) Optical molecular imaging (Cerenkov Luminescence Imaging, CLI) for diagnosis [15-21] and oxygen assessment [22,23] and 2) The Position and dosimetry verification for radiotherapies, such as electronic portal imaging [24] and image-based dosimetry applications [25-27]. Additionally, Helo Y, et al. [28] reported the feasibility of applying Cerenkov light imaging in proton therapy.

In this work, we investigate the use of Cerenkov light induced by 45MV X-rays from a LA45 accelerator to replace laser light in PDT to activate photosensitizers (5-ALA with catalase's substrate coenzyme) to produce singlet oxygen to destroy cell structure and to block the delivery of nutrition to the cell. This treatment is called Radio-Dynamic Therapy (RDT) as reported in the publications [29,30,31]. RDT overcomes the limitation of laser/visible light penetration in PDT because 45 MV X-rays can penetrate effectively through bones and soft tissues and generate Cerenkov light in deep-seated tumors.

MATERIAL AND METHODS

Theoretic Analysis

Cerenkov light is a threshold reaction for a charged particle and the threshold energy is given by

$$\beta n > 1; \quad (1)$$

Where n is the refractive index and β is defined as:

$$\beta = \sqrt{1 - \left(\frac{1}{\frac{E_{\text{keV}}}{511} + 1} \right)^2} \quad (2)$$

Cerenkov light will be emitted while the velocity of a charged particle in the media is greater than the phase velocity of light in the medium. In water, the threshold energy of electrons is 0.264 MeV. However, in tissue, the threshold energy is 0.219 MeV for a refractive index (n) of 1.4. Several radioisotopes used in biomedical imaging [15,18] satisfy the Cerenkov energy criterion in equation (1).

Further studies by Ilya Frank and Igor Tamm [32] predicted the number N of Cerenkov photons emitted within a wavelength interval in the case of $\lambda_1 < \lambda_2$ based on the path length x of an electron:

$$\frac{dN}{dK} = \frac{2\pi}{137} \left(\frac{1}{\lambda_1} - \frac{1}{\lambda_2} \right) \left(1 - \frac{1}{\beta^2 n^2} \right) \quad (3)$$

Two conclusions can be drawn from this equation: 1) higher energy particles will generate stronger Cerenkov light, and 2) the peak of Cerenkov light spectrum is between ultraviolet (UV) and blue.

A photon cannot directly produce Cerenkov light. However, Cerenkov light can be generated by secondary particles such as electrons or positrons as a result of photon interactions with a medium (Compton Effect, Pair productions, photonuclear interactions) in which the velocity of such secondary charged particles is greater than the phase velocity of light in the medium.

The LA45 Accelerator and Definition of Radio-Dynamic Therapy

In this work, Cerenkov light is induced from a high energy racetrack accelerator LA45 (Topgrade HC, Beijing, China), which can accelerate electrons up to 45MeV and produce 45 MV X-rays using a tungsten target [33]. Comparing with conventional Linacs in radiotherapy, the LA45 accelerator produces higher energy X-rays and leads to more significant Cerenkov light. Hence, it has the potential to replace laser light in PDT to activate photosensitizers to produce singlet oxygen. It is a Cerenkov- induced PDT by high-energy X-rays. To enhance the singlet oxygen production, a patented coenzyme has been added to the photosensitizers as a substrate for catalytic action. The 45MV X-rays are delivered to the tumor target using 3D conformal radiation therapy (3DCRT), 3-6Gy/fractions, 1 fraction/week, 4~6weeks. Before the 3DCRT treatment, a small dose of 5-10 cGy is delivered to the entire

body of the patient (TBI: 5-10 cGy) to initiate and stimulate the immunological response of the total body and to improve the cell function. Therefore, RDT combines Cerenkov-induced PDT and radiation therapy into one treatment modality. The main effect is believed to be from Cerenkov- induced PDT and it is further synergistically enhanced by radiation therapy. Accordingly, there are three key elements in RDT, 45MV X-rays (the LA45 accelerator), photosensitizer and patented coenzyme.

As charged particle energy increases, the intensity of Cerenkov light significantly increases. The number of electrons from a clinical accelerator is 3 to 5 orders greater than that from the isotopic β - emitters. Therefore, the number of Cerenkov light photons from a clinical accelerator is at least 2 to 3 orders higher than that from isotopic β -emitters with energies less than 1 MeV typically [34]. This may explain why Cerenkov light created by isotopic β -emitters, such as ^{18}F -FDG and Yttrium-90, is not sufficient for clinical PDT applications.

Furthermore, Cerenkov light produced from conventional Linac beams (beam energies below 15MV) is mainly by charged particles in the beam or created by direct photon interactions, e.g. Compton interactions and Pair productions, which is an instant emission, about 10-16 sec (the fast component). For 45MV photon beams from a LA45 accelerator, however, there is also a slow component due to charge particles, e.g. positrons emitted by radionuclides ^{11}C and ^{15}O produced by photonuclear reactions by 45 MV X-rays, similar to that by ^{18}F -FDG PET tracers. The slow component is a continuing emission process that may last several minutes or several hours. The emission time depends on the half-life of the radionuclides. The continuing Cerenkov light emission is beneficial to RDT. The photonuclear reactions are the threshold reactions. The photonuclear reactions in conventional clinical accelerators are very low because its x-ray energy is less than the threshold energy.

Monte Carlo Simulation

We performed MC simulations of the LA45 accelerator to obtain the energy spectra of 5 and 45MV photon beams and then simulated Cerenkov light production in a water phantom using the GEANT4 code for various energies of electrons, positrons, and photons. The Geant4 code used in this work was GEANT4 9.6.0 - Optical Photon Process - Cerenkov Effect. The dimensions of the water phantom were 30cm \times 30cm \times 30cm. Charged particles were isotropically ejected from the center of the water phantom with monoenergetic energies from 0.2 MeV to 50 MeV. The simulated particle histories (counts) were 100,000 for photons and 10,000 for positrons and electrons for

every energy level, respectively. The simulated counts for the 5 and 45 MV X-ray spectra from the LA45 accelerator were also 100,000.

RESULTS AND DISCUSSION

Monte Carlo Simulation

The simulated Cerenkov light emission from monoenergetic electrons, positrons and photons in water as a function of energy are shown in **figure 1**. The numbers of Cerenkov light photons generated by monoenergetic electrons, positrons and photons in water are also listed in **table 1**.

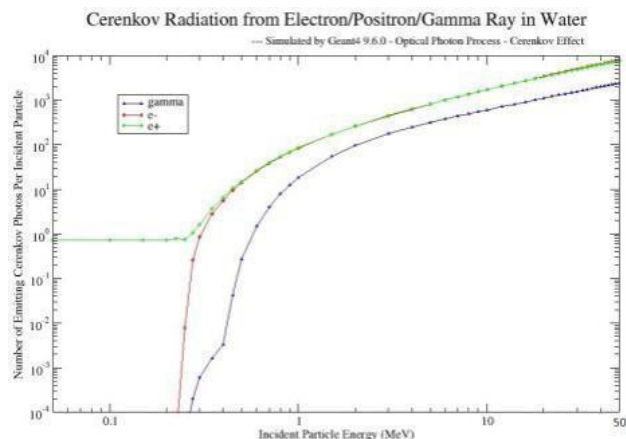


Figure 1: Cerenkov light emission from monoenergetic electrons/positrons/photons in water.

Table 1: The number of Cerenkov light photons induced by monoenergetic photons, electrons, and positrons in water.

Energy (MeV)	Photon	Electron	Positron
0.5	0.27	14.2	15.3
1.0	18.4	83.3	86.1
5.0	315.6	810.9	819.1
10.0	605.8	1719.2	1701.0
20.0	1111.1	3424.5	3344.3
50.0	2384.5	7878.8	7560.9

The energy spectra of 45/5MV X-rays from the LA 45 accelerator are shown in **figure 2 and 3**, respectively. The ratio of Cerenkov photons generated by 45MV and 5MV X-rays from the LA 45 accelerator are listed in table 2. The ratio of Cerenkov light generated by 50MeV and 5MeV monoenergetic photons in water is also listed in **table 2**.

Table 2: The ratio of Cerenkov light photons generated by 45MV and 5MV x-ray beams from the LA 45 accelerator in a water phantom and the ratio for 50MeV and 5MeV monoenergetic photons. * Monoenergetic photon.

Incident Radiation	Ratios
45/5 MV	5.54
50/5 MeV*	7.56

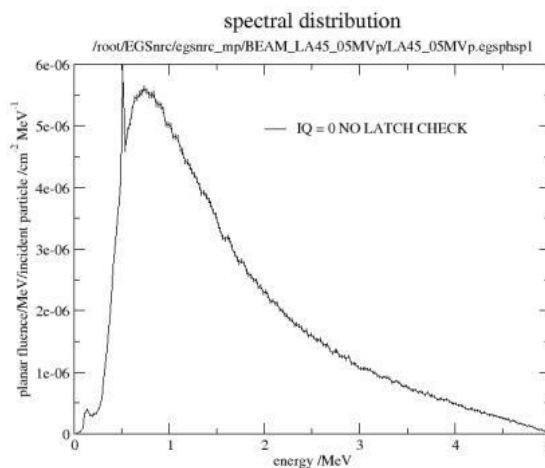


Figure 2: The energy spectrum of a 5MV x-ray beam from the LA45 accelerator.

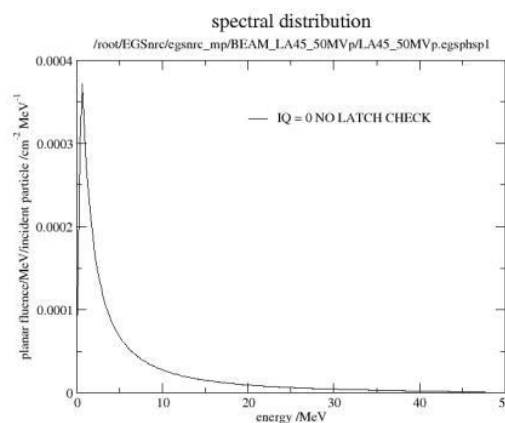


Figure 3: The energy spectrum of a 45MV x-ray beam from the LA45 accelerator.

According to figure 1, the intensity of Cerenkov light will increase with the energy of the incident particles, and, in particular, will drastically increase at lower energies (below 2 MeV). The threshold energy for electrons and photons is 0.22 MeV and 0.26 MeV, respectively. These are consistent with the results calculated from Equations (1) and (2). Since photons are not charged particles, Cerenkov light induced by photons is a result of secondary charged particles. Hence, Cerenkov light intensity by photons is less than that by the same energy electrons. However, Cerenkov light by positrons does not have a threshold. For positrons of energies < 0.22 MeV, the intensity of Cerenkov light remains unchanged. This is mainly because any positron can be annihilated with surrounding electrons and emits 0.511 MeV photons and, in turn, these photons can produce Cerenkov light through secondary charged particles from the photoelectric effect, Compton Effect, and Pair production.

The results in table 2 indicate that Cerenkov light from a 45MV x-ray beam or 50MeV monoenergetic photons is 5-8 times of that from a 5MV X-ray beam or 5MeV monoenergetic photons. This suggests that higher energy X-rays are more effective in Cerenkov light generation. The spectra of Cerenkov light

from 5 MV and 45 MV X-rays was calculated using the MC method. **Figure 4** shows the normalized spectral distributions for both X-ray beams. It shows that the intensity of Cerenkov light decreases with the wavelength from 300 to 650nm. The highest intensity of Cerenkov light is in the UV region. The normalized spectra of Cerenkov light from 5MV and 45MV X-rays are identical, which is consistent with previous observations [25,26,35,36]. As shown in figure 4, the intensity of Cerenkov light at 300nm and 400nm equals nearly 5.5 and three times the intensity at 630nm wavelength, respectively. This also suggests that radiation-induced Cerenkov light is more effective than laser light at 630nm, which is the common light source used in conventional PDT.

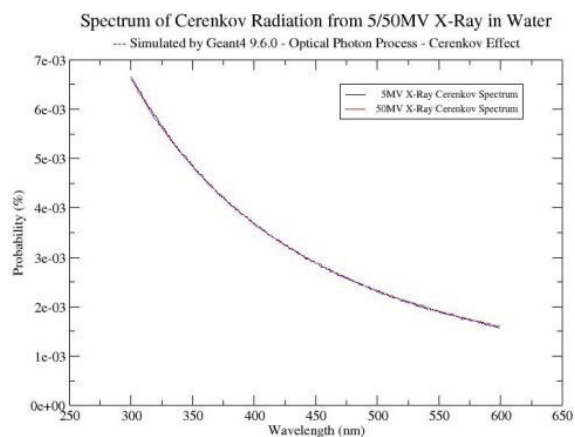


Figure 4: The normalized spectra of Cerenkov light from 5/45MV x-rays in water.

The Resonance Absorption of PPIX's to Cerenkov Light

Protoporphyrin IX (PpIX) is an endogenous photosensitizer, which shows strong absorption characteristics in the UV region, from 370nm to 430nm, and peaked at 405nm. This resonance absorption is called Soret Band [37].

PpIX is derived from the photosensitizer prodrug, 5-aminolevulinic acid (5-ALA), a precursor in the heme biosynthetic pathway. Although several photosensitizers other than 5-ALA-derived PpIX have been used in clinical PDT, 5-ALA-based PDT has garnered increased interest in clinical PDT research during the past decades. Some studies [38,39] have shown that higher accumulation of 5-ALA-derived PpIX in rapidly proliferating cells may provide a biologic rationale for the clinical use of 5-ALA-based PDT and diagnosis. Therefore, we have selected PpIX derived from the photosensitizer prodrug, 5-ALA as the photosensitizer in this work.

Figure 5 shows the excitation spectra of PpIX and the strong resonance absorption of Soret-Band at 400nm and 405 nm in methanol and tissue, respectively [39]. It is apparent that the absorption efficiency during 370- 430nm is much greater than the absorption efficiency at 630nm, which is the laser

light wavelength commonly used in clinical PDT. The peak at 400/405nm is at least 20-30 times higher than that at 630nm. As seen from 5.1, the highest intensity of radiation-induced Cerenkov light is in the UV region, overlapping with the peak excitation values for PpIX in tissue from 370nm to 430nm. By integrating the PpIX excitation values in figure 5 with the Cerenkov spectrum induced by 45MV X-rays in figure 4, we can see that radiation-induced Cerenkov light is 15 times more effective in activating PpIX than commonly used 630nm laser light.

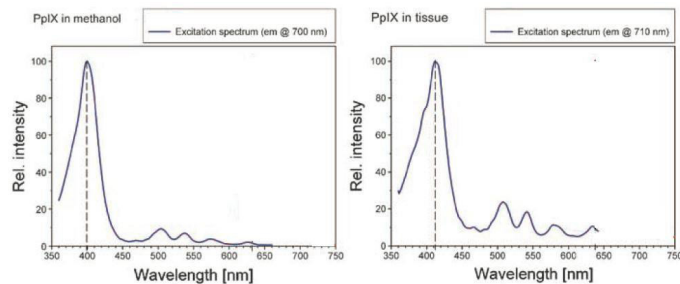


Figure 5: The excitation spectra of PpIX in methanol (left) and tissue (right), respectively 39.

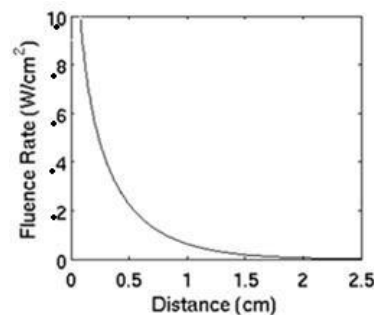


Figure 6: The fluence rate distribution in tissue as a function of the distance from the light source, which is placed at the tissue surface.

Homogeneous Inner Excitation of Photosensitizers by Cerenkov Light in RDT

In RDT, the tumor target is treated using 3DCRT with 45MV X-rays, which will create a nearly uniform X-ray dose distribution within the treatment volume. This process also results in a nearly homogeneous Cerenkov light distribution in the tumor target because Cerenkov light is generated by charged particles that also determine the X-ray dose distribution. Consequently, the excitation of photosensitizers by Cerenkov light is nearly homogeneous inside the treatment volume and, therefore, Cerenkov light can be regarded as an internal homogenous light source.

In conventional PDT, however, the tumor target is irradiated by external light from one direction and the light intensity decreases dramatically with depth. Figure 7 illustrates the fluence rate versus distance from the center of the light source, which is a 3cm diameter cylindrical source emitting 1.0W/cm² at the surface. The fluence rate distribution during

PDT was simulated using the Monte Carlo method. The optical properties of the tissue were assumed as follows: $\mu_a = 0.01 \text{ mm}^{-1}$, $\mu_s = 10 \text{ mm}^{-1}$, $g = 0.9$ and the tissue index of refraction = 1.4. At a depth of 7 mm under the the skin surface, the intensity of light decreases to about 10% of that at the skin surface. This depth is often the maximum treatment depth for superficial tumors in PDT.

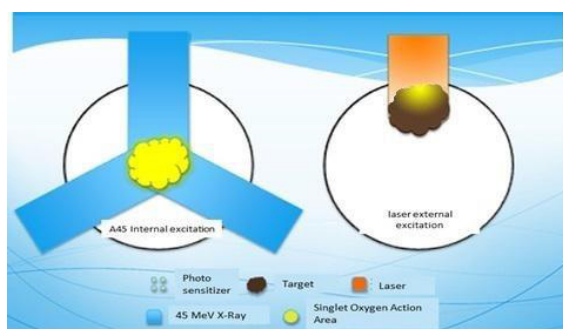


Figure 7: The comparison of the photosensitizer excitation effects by the internal Cerenkov light from 45MV x-rays in RDT and by the external laser light in PDT.

Figure 8 shows the main difference in the excitation process between RDT and conventional PDT. For RDT, as mentioned above, the excitation of photosensitizers is achieved by the internal homogeneous Cerenkov light in the tumor target irradiated by 45MV X-rays. There is little difference between shallow tumors or deep-seated tumors in the body because of the penetrability of 45MV X-rays. For PDT, however, because of the nearly exponential decrease of external laser light, the laser intensity requirement for PDT is determined by the deepest depth of the tumor target. For example, to ensure complete tumor cell killing at a depth of 7mm, the laser intensity at the skin surface has to be 10 times higher than that at a depth of 7mm below the skin surface. For RDT, in contrast, the internal Cerenkov light is homogeneous and, therefore the light intensity requirement will be 10 times less for a 7mm thick tumor in PDT. More importantly, PDT cannot effectively treat tumors beyond a 7mm depth under the skin surface while RDT can treat deep-seated tumors anywhere in the body. Moreover, because of its shorter wavelengths and the possibility to be generated inside a given cell, the Cerenkov light has much better absorption/excitation properties at the microscopic level [40], which may be very helpful in killing cancer cells. Finally, Cerenkov light generated by 45MV X-rays has both a fast component and a slow component and the latter is a continuing emission process lasting about 2-20 minutes. The radiobiological effect of this slow component on tumor cell killing remains unknown at the moment.

The Catalyst Effect of the Substrate Coenzyme

In RDT, a coenzyme has been added as a substrate to

photosensitizer 5-ALA to catalyze more singlet oxygen. In an early work [41], the catalytic conversion of specific H_2O_2 into $^1\text{O}_2$ by PpIX was investigated for high-energy x-ray irradiation. A fluorescent marker DMA (9, 10- dimerthylanthracence) was used to quantify the singlet oxygen production. Historically, in addition to the fluorescent marker DMA, singlet oxygen sensor green reagent (SOSG) was also used for testing whether some chemicals or coenzymes could enhance the entire reaction [42]. In this study, the production of singlet oxygen $^1\text{O}_2$ was monitored with $2.12 \mu\text{M}$ DMA.

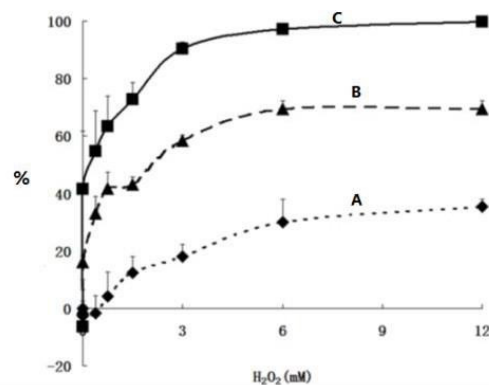


Figure 8: The effects of irradiation and specific H_2O_2 on the production of $^1\text{O}_2$ in the presence of $14.4 \mu\text{M}$ of PpIX and $1.05 \mu\text{M}$ of DMA: (A) without x-ray irradiation, (B) with 1Gy x-ray radiation using 6MV beams and (C) using 45 MV beams.

Figure 8 shows the effect of specific H_2O_2 on the production of singlet oxygen. When more coenzyme H_2O_2 was added, more singlet oxygen was generated. With additional 3mM H_2O_2 and 1 Gy of 45MV X-ray irradiation, more than 90% of PpIX was transferred to singlet oxygen. It plateaued with 4-6mM coenzyme and 1 Gy of 45MV X-ray radiation. Without radiation, the production of singlet oxygen also increased with the H_2O_2 concentration and reached a stable state of 20- 30%. The results showed that (1) the amount of PpIX transferred to singlet oxygen with specific H_2O_2 added was 2.5-5 times compared to that without catalytic coenzyme added, and (2) the amount of PpIX transferred to singlet oxygen with 45MV irradiation was 3-5 times of that without irradiation (in the presence of only catalytic coenzyme and PpIX).

The Combined Effects of Cerenkov-Based PDT and Radiation Therapy

The biological response of PDT depends not only on the local light intensity but also on the fluence rate and treatment time, i.e. the light dose and dose rate. In previous experiments [22], the intensity of Cerenkov light induced by 6MV and 18MV X-rays from a Varian 2100C accelerator was investigated. At a dose rate of 4Gy/min, the fluence rate of Cerenkov light generated by 6MV and 18MV X-rays in muscle tissues was $0.7 \times 10^{-3} \text{ mW/cm}^2$ and $1.1 \times 10^{-3} \text{ mW/cm}^2$, respectively. Based

on previous experiments and our Monte Carlo simulations, Cerenkov light by 45MV X-rays was 5-8 times more than that by 5MV X-rays. This means that the possible fluence rate of Cerenkov light generated by 45MV X-rays from the LA45 accelerator is about $3.5\text{-}5.6 \times 10^{-3}\text{mW/cm}^2$ (at a dose rate of 4Gy/min). This is much lower than that used in conventional PDT [1,39], which is about $1\sim 10^2\text{mW/cm}^2$.

However, some unique characteristics of Cerenkov-induced PDT will lower the fluence rate requirement for RDT: (1) the higher efficiency of Cerenkov light to activate PpIX, i.e. the Soret-Band Effect, a factor of 10-20 improvements, (2) the homogeneous internal activation, a factor of 10 improvements, and (3) the coenzyme catalysis, a factor of up to 5 improvements. These combined improvements (up to 1000 times) indicate an equivalent excitation fluence rate of up to 5mW/cm^2 with Cerenkov-induced PDT. This equivalent fluence rate is within the range of $1\sim 10^2\text{mW/cm}^2$ for conventional PDT using the 630nm laser light. Therefore, Cerenkov-induced PDT may have comparable biological response and fluence rate effects as conventional laser light-based PDT.

During a complete RDT treatment course, the tumor target is treated with 3DCRT using 45MV X-rays to a total dose of 18-36Gy (3-6Gy/fractions, 1fraction/week, 4~6weeks). Although this dose is insufficient to evacuate all of the tumor cells, it is expected to have a synergetic effect with the outcome of Cerenkov-induced PDT. Radiation therapy with large fractioned doses is intended to debulk large tumor masses, which are often hypoxic with poor vasculature, and to improve the therapeutic efficacy of PDT through better photosensitizer circulation/absorption in the tumor tissues. The equivalent light dose for Cerenkov-induced PDT using the maximum radiation dose of 36Gy and the estimated fluence rate of 5mW/cm^2 is 2.7J/cm^2 , which is still lower than the light dose in conventional laser light-based PDT of $10\text{-}100\text{J/cm}^2$. However, the combined therapeutic effect of Cerenkov-induced PDT and radiation therapy may provide a sufficient tumorsidal dose for cancer therapy. Additionally, there is also a therapeutic contribution from continuous activation of PpIX to singlet oxygen due to the slow Cerenkov light generation, which lasts several tens of minutes by 45MV X-rays. Further experimental and clinical studies are warranted to confirm the dosimetric requirements for RDT.

Recently, some research studies on low-level light phototherapy [3,7,40,43,44] could shed light on the mechanism of RDT. For example, Mathews MS, et al [45] showed that effective ALA-PDT decreased cell viability or inhibited spheroid growth at

low light dose and fluence rates (light dose 1.5, 3, or 6J/cm^2 ; irradiance = $0.017\text{-}17\text{mW/cm}^2$) if given over long periods. The work by Bisland SK, et al. [46] showed the use of low fluence rates (irradiance = 0.116mW/cm^2) and long exposures (1-4 days) has notably increased selective apoptosis (programmed cell death) of tumor cells, which is more desirable when compared to the inflammation and edema that commonly occur with the uncontrolled rupturing of cellular contents of necrosis.

CONCLUSIONS

Our results and detailed discussions indicate that the PpIX excitation process and the efficiency of RDT using Cerenkov light from 45MV X-rays is similar to that using the 630nm laser light in conventional PDT. Comparing the mechanisms and therapeutic effect of RDT with conventional PDT, RDT brings a synergetic action, a combination of Cerenkov-induced PDT and hypofractionated radiation therapy. RDT may be developed into a potential treatment modality for a wide range of cancers and various cancer stages as well as for other diseases.

DISCLOSURE OF CONFLICTS OF INTEREST

The authors have no relevant conflicts of interest to disclose.

REFERENCES

1. Wilson BC, Patterson MS (2008). The physics, biophysics, and technology of photodynamic therapy. *Physics in medicine and biology*. 53: R61-109.
2. Achilefu S, Raghavachari R, SPIE (Society). (2012). Reporters, markers, dyes, nanoparticles, and molecular probes for biomedical applications IV: 23-25 January 2012, San Francisco, California, United States. Bellingham, Wash. SPIE. 23-25.
3. Kotagiri N, Sudlow GP, Akers WJ, Achilefu S. (2015). Breaking the depth dependency of phototherapy with Cerenkov light and low-radiance-responsive nano photosensitizers. *Nature Nanotechnology*. 10(4): 370-379.
4. Michael WN, Tracy LG. (2015). Activation of psoralen at depth using kilovoltage X-rays: physics considerations in implementing a new teletherapy paradigm. *Med Phys*. 42: 3352.
5. Pritikin J, Weinman D, Harmatz A, Young H. (1992). Endoscopic laser therapy in gastroenterology, *The Western journal of medicine*. 157: 48-54.
6. Mallidi S, Anbil S, Bulin AL, Obaid G. (2016). Beyond the Barriers of Light Penetration: Strategies, Perspectives,

- and Possibilities for Photodynamic Therapy. *Theranostics*. 6(13): 2458-2487.
7. Hartl BA, Hirschberg H, Cherry S. (2016). Activating Photodynamic Therapy In Vitro with Cerenkov light Generated from Yttrium-90. *J Environ Pathol Toxicol Oncol*. 35(2): 185-192.
 8. Glaser AK, Zhang R, Andreozzi JM, Gladstone AJ, et al. (2015). Cerenkov light fluence estimates in tissue for molecular imaging and therapy applications. *Phys Med Biol*. 60: 6701–6718.
 9. Ma L, Zou X, Chen W. (2014). A New X-Ray Activated Nanoparticle Photosensitizer for Cancer Treatment. *J Biomed Nanotechnol*. 10: 1501–1508.
 10. Yao M, Ma L, Li L, Zhang J, et al. (2016). A New Modality for Cancer Treatment—Nanoparticle Mediated Microwave Induced Photodynamic Therapy. *J Biomed Nanotechnol*. 12: 1835–1851.
 11. Chen W, Zhang J. (2006). Using Nanoparticles to Enable Simultaneous Radiation and Photodynamic Therapies for Cancer Treatment. *J Nanosci Nanotechnol*. 6: 1159–1166.
 12. Wang C, Cheng L, Liu Z. (2013). Upconversion Nanoparticles for Photodynamic Therapy and Other Cancer Therapeutics. *Theranostics*. 3: 317-30.
 13. Haase M, Schäfer H. (2011). Upconverting Nanoparticles. *Angew Chem Int Ed Engl*. 50(26): 5808–5829.
 14. Cerenkov PA. (1934). Visible Emission of Clean Liquids by Action of Gamma Radiation. *Dokl Akad Nauk. SSSR* 2: 451–454.
 15. Li C, Mitchell GS, Cherry SR. (2010). Cerenkov luminescence tomography for small-animal imaging. *Optics Letters*. 35: 1109-11.
 16. Liu H, Ren G, Miao Z, Zhang X, et al. (2010). Molecular optical imaging with radioactive probes. *PloS one*. 5(3): e9470.
 17. Mitchell GS, Gill RK, Boucher DL, Li C, et al. (2011). In vivo Cerenkov luminescence imaging: a new tool for molecular imaging *Philosophical Transactions Series A. Mathematical, physical, and engineering sciences*. 369: 4605-19.
 18. Robertson R, Germanos MS, Li C, Mitchell GS, et al. (2011). Multimodal imaging with (18)F-FDG PET and Cerenkov luminescence imaging after MLN4924 treatment in a human lymphoma xenograft model. *J Nucl Med*. 52(11): 1764-9.
 19. Ruggiero A, Holland JP, Lewis JS, Grimm J. (2010). Cerenkov luminescence imaging of medical isotopes. *Journal of nuclear medicine: official publication. Soc Nucl Med*. 51: 1123-30.
 20. Spinelli AE, D'Ambrosio D, Calderan L, Marengo M, et al. (2010). Cerenkov light allows in vivo optical imaging of positron-emitting radiotracers. *Physics in medicine and biology*. 55: 483-95.
 21. Tanha K, Pashazadeh AM, Pogue BW. (2015). Review of biomedical Čerenkov luminescence imaging applications. *Biomed Opt Express*. 6(8):3053.
 22. Axelsson J, Davis SC, Gladstone DJ, Pogue BW. (2011). Cerenkov light induced by external beam radiation stimulates molecular fluorescence. *Medical physics*. 38: 4127-32.
 23. Axelsson J, Glaser AK, Gladstone DJ, Pogue BW. (2012). Quantitative Cerenkov light spectroscopy for tissue oxygenation assessment. *Optics express*. 20: 5133-42.
 24. Mei X, Rowlands JA, Pang G. (2006). Electronic portal imaging based on Cerenkov light: a new approach and its feasibility. *Medical physics*. 33: 4258-70.
 25. Zhang R, Fox CJ, Glaser AK, Gladstone DJ, et al. (2013). Superficial dosimetry imaging of Cerenkov light in electron beam radiotherapy of phantoms. *Physics in medicine and biology*. 58: 5477-93.
 26. Zhang R, Glaser AK, Gladstone DJ, Fox CJ, et al. (2013). Superficial dosimetry imaging based on Cerenkov light for external beam radiotherapy with the megavoltage x-ray beam. *Medical physics*. 40(10): 1914-26.
 27. Zlateva Y, Naqa IE. (2015). 2015 BEST IN PHYSICS (THERAPY): Cerenkov light Dosimetry: Feasibility for Electron Radiotherapy. *Med Phys*. 42: 3567-3567. MO-FG-303-02.
 28. Helo Y, Kasperek A, Rosenberg I, Royle G, et al. (2014). The physics of Cerenkov light production during proton therapy. *Physics in medicine and biology*. 59: 7107-23.
 29. Zhang QS, Sun QY, Xiao GP, Zeng J, Chen L and Ma CM. (2016). The Mechanism Research of Radio-Dynamic Treatment, *Radiat Oncol*, 119: s907.
 30. Zhang QS, Sun QY, Xiao GP, Zeng J, et al. (2016). Research Work of the Radio-Dynamic Treatment Mechanism, *Med Phys*. 43: 3826-3827.
 31. Zhang QS, Sun QY, Xiao GP, Zeng J, Mu X, Chen L, and Ma CM. (2018). Radio-Dynamic Therapy (RDT) Combining Cerenkov-Induced PDT and RT, *Int J Radiat Oncol Biol Phys*. 99: E592-E592.
 32. Frank I, Tamm I. (1937). Coherent visible radiation of fast electrons passing through matter *CR(Dokl) Acad Sci URSS*. 14: 109-14.
 33. Zhang QS, Yiming H, Yun L, et al. (2012). Study of in situ photonuclear reaction $^{16}\text{O} \gamma \gamma \text{ } ^{15}\text{O}$ using 45MV bremsstrahlung for hypoxia PET imaging in tumor. *Chinese Journal of Medical Physics*. 29 (4): 3472-3477.
 34. Glaser AK, Zhang R, Andreozzi JM, Gladstone AJ, et al.

- (2015). Cerenkov light fluence estimates in tissue for molecular imaging and therapy applications. *Phys Med Biol.* 60:6701–6718.
35. Zhang R, Fox CJ, Jarvis LA, Gladstone DJ. (2015). BEST IN PHYSICS (IMAGING) Superficial dose imaging based on Cerenkov light emission during megavoltage external beam radiotherapy. *Medical physics.* 40: 524.
36. Zhang R, Gladstone DJ, Jarvis LA, Strawbridge RR, et al. (2013). Real-time in vivo Cherenkovscopy imaging during external beam radiation therapy. *Journal of biomedical optics.* 18(11): 504-7.
37. Sano S, Rimington C. (1960). Spectral-absorption coefficients of some porphyrins in the Soret-band region. *Biochemical Journal.* 75: 620-23.
38. Peng Q, Warloe T, Berg K, Moan J, et al. (1997). 5-Aminolevulinic acid-based photodynamic therapy. Clinical research and future challenges. *Cancer.* 79(12): 2282-308.
39. Reinhold B, Barbara K, Roy P, Herbert S. (2006). *Photodynamic Therapy with ALA: A Clinical Handbook.* Royal Society of Chemistry.
40. Hartl BA, Hirschberg H, Marcu L, Cherry SR. (2015). Characterizing low fluence thresholds for in vitro photodynamic therapy. *Biomed Opt Express.* 6(3): 770–9.
41. Zeng J, Sun Q, Su J, Han J, et al. (2015). Protoporphyrin IX catalyzed hydrogen peroxide to generate singlet oxygen. *International journal of clinical and experimental medicine.* 8: 6829- 34.
42. Michael FL. (2007). *Radioactivity Introduction and History.* Oxford.
43. Farrell TJ, Wilson BC, Patterson MS, Olivo MC. (1998). Comparison of the in vivo photodynamic threshold dose for photofrin, mono- and tetrasulfonated aluminum phthalocyanine using a rat liver model *Photochem. Photobiol.* 68: 394–9.
44. Gonzales J, Wang F, Zamora G, Trinidad A, et al. (2014). Ultra-low fluence rate photodynamic therapy: simulation of light emitted by the Cerenkov effect. *Proc. SPIE.* 89280F–11.
45. Mathews MS, Angell-Petersen E, Sanchez R, Sun CH, et al. (2009). The Effects of Ultra-Low Fluence Rate Single and Repetitive Photodynamic Therapy on Glioma Spheroids. *Lasers in Surgery and Medicine.* 41:578–584.
46. Bisland SK, Lilge L, Lin A, Rusnov R, et al. (2004). Metronomic photodynamic therapy as a new paradigm for photodynamic therapy: rationale and preclinical evaluation of technical feasibility for treating malignant brain tumors. *Photochem Photobiol.* 80(1): 22–30.